Molecular Dynamics and Structure of the Random Coil and Helical States of the Collagen Peptide, α1-CB2, as Determined by ^{13}C Magnetic Resonance†

D. A. Torchia,* J. R. Lyerla, Jr.,‡ and A. J. Quattrone

ABSTRACT: Carbon-13 chemical shifts, spin-lattice (T_1) and spin-spin (T_2) relaxation times, and ^{13}C-{^1H} nuclear Overhauser enhancements (NOE) have been determined for the random coil and triple helical states of the α1-CB2 fragment of rat skin collagen. Assignment of all aliphatic resonances of this 36 residue peptide in the random coil state (30°) has been achieved with the aid of model polypeptides containing pyrrolidine residues. The chemical shifts and intensities of the Pro and Hyp C^γ resonances show that ≳90% of the X-Pro and X-Hyp bonds are trans in both helix and coil conformations. From T_1 measurements rotational correlation times (τ_{eff}) of *ca.* 0.45 nsec are calculated for interior C^α carbons in the coil, while τ_{eff} values of the side chain and near terminal carbons are found to be 2–9 times smaller. These results along with the narrow natural line widths (3–5 Hz) and maximal NOE values (2.8 ± 0.3) demonstrate the high degree of backbone mobility, due to segmental motion, in the unordered state of the peptide. By contrast, the broad lines (50–90 Hz) and small NOE values (1.3 ± 0.3) for the α carbons in the helical state (2°) suggest much slower motion. The line widths and NOE values together with the C^α T_1 values (0.025–0.040 sec) correspond to correlation times which are in reasonable agreement with those calculated for an axially symmetric rigid ellipsoid, undergoing rotational diffusion, having dimensions approximating those of a collagen-type triple helical aggregate of three α1-CB2 chains. A satisfactory computer simulation of the experimental 2° spectrum is obtained by assigning the narrow aliphatic resonances in the spectrum (line widths 5–40 Hz) to (a) carbons in the small amounts of α1-CB2 (3 mol %) and α1-CB1 (2.5 mol %) random coil conformations, (b) carbons in the flexible terminal triplets of the helix, and (c) Ala, Leu, and Phe methyl and phenyl carbons. The side chain carbon line widths obtained from the simulation—when compared with side chain line widths calculated for a rotating rigid ellipsoid with internal motion—indicate rapid axial reorientation of methyl and phenyl groups. With the exception of the Hyp residue the line widths suggest local motion for at least some carbons in most other side chain moieties. The Hyp C^β and C^γ line widths indicate the presence of little if any rapid Hyp ring motion.

The primary biological function of collagen, the major protein constituent of connective tissue and bone, is structural. The structural unit common to all collagens at the molecular level is the triple stranded helix. Each of the three α chains which comprise the helix consists of *ca.* 1000 amino acids. The stability of the helical structure results from the regular amino acid sequence of the α chains which consist of Gly-X-Y[1] triplets where X and Y are often pyrrolidine residues. The regularity of the α-chain sequence has prompted many model studies (Traub and Piez, 1971; Sakakibara *et al.*, 1973) using synthetic peptides of the form $(Gly\text{-}X\text{-}Y)_n$. Recent advances in collagen chemistry have permitted model studies using small fragments of the α chains themselves (Piez and Sherman, 1970a,b; Ward and Mason, 1973). One such fragment, α1-CB2, obtained from the α1 chain of rat skin collagen has 36 residues in the sequence[2] (Bornstein, 1967)

Gly-Pro-Ser-Gly-Pro-Arg-Gly-Leu-Hyp-Gly-Pro-Hyp-Gly-Ala-Hyp-Gly-Pro-Gln-Gly-Phe-Gln-Gly-Pro-Hyp-Gly-Glu-Hyp-Gly-Glu-Hyp-Gly-Ala-Ser-Gly-Pro-Hse

and undergoes a temperature induced reversible transition from a random coil to a rod-like triple-stranded structure (trimer) of high (~90%) helix content (Piez and Sherman, 1970a,b).

It was anticipated that the conformations of this peptide could be further elucidated using ^{13}C nuclear magnetic resonance (nmr) spectroscopy, since resonances due to carbons in different residues can be resolved in complex peptides (Lyerla and Freedman, 1972). Although the low abundance (1.1%) of ^{13}C nuclei gives rise to weak signals, sensitivity enhancement is provided using Fourier transform techniques (Farrar and Becker, 1970) which also enable spin-lattice relaxation times (T_1) to be readily measured (Vold

† From the Polymers Division, National Bureau of Standards, Washington, D.C. 20234 (D.A.T. and J.R.L., Jr.) and the Laboratory of Biochemistry, National Institutes of Dental Health, Bethesda, Maryland (A.J.Q.). *Received August 19, 1974.* This work was supported, in part, by the National Institutes of Dental Research under Interagency Agreement Y01-DE-30013. A preliminary report of this work has been presented (Torchia *et al.*, 1974a).

*Address correspondence to this author at National Institutes of Health Building 30, Room 106, Bethesda, Md., 20014.

‡ NRC-NAS Postdoctoral Research Associate.

[1] Abbreviations used are: X, residue in position 2 of the triplet; Y, residue in position 3 of the triplet; FID, free induction decay; *K*, 1024; C′, the backbone carbonyl carbons; NOE, the ^{13}C-{^1H} nuclear Overhauser enhancement; ω_H and ω_C, the respective Larmor frequencies of the ^{13}C and ^1H nuclei; 2a and 2b, the respective major and minor axes of the ellipsoid of revolution; $\rho = b/a$; R_1 and R_2 for the respective diffusion coefficients for rotation about the major and minor axes of the ellipsoid; $\sigma = R_1/R_2$; $\tau_A = 1/(6R_2)$; θ, the angle between a given C–H bond and the major axis of the ellipsoid; $\theta_H{}^\alpha$, the angle between a C^α–H^α bond and the major axis; χ^i, the rotation angle about the *i*th side chain bond; $R_\chi i$ for the rate of rotation about bond *i*; Hse, homoserine.

[2] Due to incomplete hydroxylation, rat skin α1-CB2 contains *ca.* 5 Hyp residues (Bornstein, 1967). Amino acid analysis showed that the sample used in this work contained 5.5 Hyp and 6.5 Pro residues.

et al., 1968). Furthermore, spin-spin relaxation times (T_2) can be estimated from ^{13}C line widths and the ^{13}C-{^1H} nuclear Overhauser enhancement (Kuhlmann *et al.*, 1970) (NOE) can be obtained from a comparison of ^{13}C signal intensities with and without proton decoupling. These nmr parameters are sensitive functions of the rotational reorientation of individual C–H (internuclear) vectors (Solomon, 1955; Abragam, 1961; Woessner, 1962; Woessner *et al.*, 1969; Allerhand *et al.*, 1971; Schaefer and Natusch, 1972). In order to determine rotational correlation times or rotational diffusion coefficients from the measured parameters (T_1, line width, NOE) it is necessary to assume a model for the reorientation of the molecule. The reorientation of globular proteins is often assumed to be represented by rotational diffusion of a sphere; however, such a model is clearly inappropriate in the case of the rod-like α1-CB2 helix. An ellipsoid of revolution approximates the shape of the α1-CB2 helix and a theoretical framework is available for relating the measured nmr parameters to rotational diffusion coefficients of the ellipsoid. Parameters which enter the theoretical expressions—the dimensions of ellipsoid model of the α1-CB2 helix and the angles made by the various C–H vectors and the long axis of the helix—can be obtained from the structures of collagen and model polypeptides determined by X-ray diffraction data (Ramachandran, 1967; Traub and Piez, 1971).

Unlike the helix, the random coil does not have a rigid conformation and exhibits complex molecular dynamics in which the reorientation of a C–H vector is characterized by a distribution of correlation times (Connor, 1963). Since detailed theoretical models for C–H reorientation in flexible polypeptide chains are not available it is not possible to relate the measured T_1 values to precisely defined correlation times. However, average or effective correlation times (τ_{eff}) (Woessner, 1962) can be calculated from measured T_1 values and do provide a reasonable description of the motion of Pro, Hyp, and Gly residues in random coiling copolypeptides composed of these residues (Torchia and Lyerla, 1974). Hence, it is anticipated that average mobility of carbons in various residues in the random coil can be determined and compared with the mobility of carbons in the helix.

While relaxation times provide information on molecular motion, chemical shifts can be used to study various features of molecular structure. In polypeptides containing pyrrolidine residues, X-Pro and X-Hyp peptide bonds are commonly cis (Bovey *et al.*, 1972; Torchia and Lyerla, 1974). Intensities and chemical shifts of pyrrolidine ring carbons can be used to determine the population of the peptide isomers in polypeptides (Dorman and Bovey, 1973; Torchia *et al.*, 1974b). Pro and Hyp resonances in the spectra of α1-CB2 have been examined for evidence of cis isomers.

Experimental Section

Preparation of α1-CB2. Collagen was extracted with a salt solution from the skins of Sprague-Dawley rats which were fed a diet containing 0.1% of β-aminopropionitrile fumarate for 3 weeks. The extracted collagen was separated into its component α and β chains using carboxymethylcellulose chromatography (Bornstein and Piez, 1966). Following cleavage of the α1 chain with cyanogen bromide (Epstein *et al.*, 1971), the resulting peptides were lyophilized to yield eight samples, each containing 200–300 mg of material. Each sample was dissolved in 5 ml of 0.5 N acetic acid at 50° and the peptides were desalted and partially fractionated by molecular sieve chromatography at room temperature on a 2.2 × 110 cm column of Bio-Gel P6 (100–200 mesh, Bio-Rad Laboratories[3]) equilibrated with 0.1 N acetic acid at 50 ml/hr. In a typical chromatograph, the first 125 ml were discarded for lack of absorbance at 236 nm. Two ensuing fractions of 115 ml were collected and lyophilized to give salt free peptide mixtures. The second fraction (*ca.* 100 mg) was resolved into the low molecular weight α1 cyanogen bromide peptides by phosphocellulose chromatography (Bornstein and Piez, 1966). Lyophilized material containing α1-CB2 was dissolved in 0.5 N acetic acid at 50° and applied to a 1.8 × 110 cm column of Bio-Gel P10 (100–200 mesh, Bio-Rad Laboratories[3]) equilibrated with 0.1 N acetic acid (17 ml/hr) at room temperature. A minor amount of cross-contamination with α1-CB1 was essentially eliminated by this procedure. The main fraction was lyophilized to a white powder; total yield of α1-CB2 was 35 mg. The sample had the predicted α1-CB2 amino acid composition, except for the presence of small amounts of aspartic acid, valine, and lysine in the hydrolysates which indicated slight contamination of the sample with α1-CB1 (*ca.* 1% by weight). The presence of less than 0.01 residue/mol of isoleucine threonine, and histidine, which are absent from α1-CB1 and α1-CB2, indicated that insignificant amounts of other peptide or protein material were present.

Model Peptides. Poly(Pro-Gly), poly(Hyp-Gly), poly(Gly-Gly-Pro-Gly), poly(Ala-Pro-Ala), and poly(Pro-Pro-Ala) were generously provided by Professor D. F. DeTar. Their syntheses and properties have been described (Mattice and Mandelkern, 1971). Poly(Pro-Ser-Gly) and poly(Ser-Pro-Gly) were the kind gifts of Dr. A. di Corato and Professor E. R. Blout who have described their syntheses and properties (Brown *et al.*, 1972). Ac-Hse-OH-lactone was prepared by reacting CNBr with Ac-Met-OH (Cyclo Chemical Co,[3]) following the procedure of Inglis and Edman (1970). Spontaneous hydrolysis of the lactone in aqueous solution (0.15 M AcONa, pH 4.8) yielded Ac-Hse-OH and was followed using ^{13}C spectroscopy.

^{13}C Fourier Transform Spectra. The 15.08-MHz ^{13}C "homebuilt" spectrometer described previously (Farrar *et al.*, 1972; Torchia and Lyerla, 1974) was used to obtain all spectra. Constant sample temperature was maintained using a Dewared probe (built at the National Bureau of Standards by Dr. D. VanderHart and Dr. H. M. McIntyre) in conjunction with a Varian[3] temperature controller. The pulse power delivered to the single coil probe was sufficient to rotate the ^{13}C magnetization by 90° in 2.5 μsec.

Unless otherwise noted, all ^{13}C results were obtained using a single solution of α1-CB2 (35 mg in 1.4 ml of aqueous (H_2O) 0.15 M AcONa, pH 4.8) contained in a 10-mm sample tube. A vortex plug kept the entire (spinning) solution volume within the transmitter-receiver coil. Since the measured T_1 values of all α1-CB2 carbons were less than 2 sec, dissolved oxygen was not removed from the solution. The solution contained approximately 4 μl of acetonitrile, 90% ^{13}C enriched at the methyl carbon, and the methyl resonance (191.7 ppm, relative to external CS_2) served as an

[3] Certain commercial companies and equipment are identified in this paper in order to specify adequately the Experimental Procedure. In no case does such identification imply recommendation or endorsement by the National Bureau of Standards, nor does it imply that the company or equipment identified is necessarily the best available for the purpose.

internal reference. The position and width of the acetonitrile resonance also served as sensitive monitors of the magnetic field homogeneity and stability during the long accumulation times required to obtain the spectra. Approximately every 12 hr a 10-mm tube containing a thermocouple immersed in a 0.15 M AcONa solution was inserted in the probe and the temperature was determined. Helix spectra were disregarded if the measured temperature fell outside the 0–4° range. Since the experiments extended over several months, a trace of sodium azide (*ca.* 1 μg) was added to the solution to inhibit bacterial growth. Except for the slow hydrolysis of the C-terminal Hse-OH-lactone to Hse-OH, no changes in composition were evident from the nmr spectra. The melting curve, obtained after completion of the nmr experiments using a Cary 60 spectropolarimeter in the ORD mode, was in agreement with that reported by Piez and Sherman (1970b).

After concluding the nmr and optical measurements of α1-CB2 in the 1.4 ml of 0.15 M AcONa (pH 4.8) solution, the pH of the solution was reduced to 1.5 by adding aliquots of 1 N HCl. The solution was then lyophilized and the resulting sample dissolved in 1.4 ml of distilled water. This lyophilization procedure was repeated five times with the pH and salt concentration finally adjusted to 4.8 and 0.15 M by adding aliquots of 0.1 N NaOH and 1 N NaCl to the solution. The nmr spectrum of this solution showed that (a) the sample was free of detectable acetate methyl and carboxyl resonances and (b) the low pH treatment used to remove the acetate effected virtually complete conversion of the C-terminal Hse-OH to Hse-OH-lactone.

Data Acquisition and Analysis. Free induction decays (FID) were accumulated in a Nicolet[3] 1080 data system using spectral windows of 4000 or 8065 Hz. Digital resolution of the transformed spectra was 2 Hz/channel. Usually, 32K FID were accumulated in the 1080 memory, and were then stored on a disk. This procedure was repeated until the desired number of FID were accumulated, and prevented loss of more than 32K FID due to spectrometer failure. The accumulated FID was digitally filtered with a time constant equal to 0.125 sec to improve the signal to noise ratio at the expense of 2.5 Hz added line width. Constant and linear phase corrections were applied, after transforming, using Nicolet[3] software programs. The random coil spin–lattice relaxation times were calculated from the integrated intensities of resonances in the inversion-recovery spectra as described by Torchia and Lyerla (1974). As noted in the text, the T_1 values of the resonances in the 2° spectrum were determined by computer simulation of the inversion-recovery spectra.

Calculated Spectra. Computer simulations of measured spectra were made using a Univac[3] 1108 digital computer, using a machine program which calculated and then summed a predetermined number of Lorentzian lines. As input, the program required the chemical shift, intensity, and line width at half-maximum of each resonance. In calculating the random coil spectrum, the chemical shift values were initially estimated from results in the literature and in Table I, and intensities were obtained from the amino acid composition. Since the motional narrowing condition was satisfied, natural line widths were estimated from the measured T_1 values using the relation, line width $= 1/(\pi T_2) = 1/(\pi T_1)$. The total line width was then taken as $1/(\pi T_2)$ + 2.5 Hz (due to digital broadening) + 2.0 Hz (due to field inhomogeneity and drift during acquisition, as estimated from the acetonitrile line width).

The helix spectrum was simulated using essentially the same chemical shifts used to calculate the coil spectrum. However, the intensities of the helix resonances were not always proportional to the number of carbons contributing to the resonance, since the mobile near terminal and side chain carbons have larger NOE values than the rigid backbone carbons. Once the helix intensities were determined from the simulation the partially relaxed spectra were calculated assuming the intensity of each resonance was given by

$$I = I_0(1 - 2\exp(-t/T_1)).$$

where I_0 is the intensity determined from the simulation of the completely relaxed spectrum (Figure 4e), t is the time between the 180° and 90° pulses and T_1 is the spin–lattice relaxation time. The T_1 values of the helix resonances were varied until satisfactory simulations of the inversion-recovery spectra, Figure 6, were obtained.

Calculation of the θ Angles. The angles between the C–H and the C–C bonds and the long axis of the helix were calculated assuming that the conformation of the α1-CB2 backbone is the same as that found for the poly(Gly-Pro-Pro) triple helix (Traub and Piez, 1971). The coordinates of the first three residues, Gly_1-Pro_2-Pro_3, in the polymer are sufficient to calculate the required angles, since all triplets have equivalent conformations with respect to the helix axis. The angles of interest were calculated using a machine program which computed the angle between the long axis of the helix and the C–D bond in the moiety

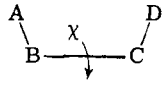

as a function of the dihedral angle χ. As input, the program required the coordinates of atoms A, B, C and the angle BCD (assumed to be 109.5°). The calculation employs standard transformation matrix techniques (Goldstein, 1950) in a procedure similar to that of Ramachandran and Sasisekharan (1968).

Results and Discussion

Random Coil Assignments. The ^{13}C Fourier transform spectra of the random coil form of α1-CB2, shown in Figure 1b, closely resembles that of denatured calf tendon collagen (Torchia and Piez, 1973), and has narrow resonances due to the rapid segmental motion in the unstructured chains. The general classification of the resonances (given in the figure) is readily made on the basis of polypeptide assignments in the literature (Christl and Roberts, 1972). With the exception of the C′ resonances, each resonance can be assigned to specific carbons in the chain, since carbon chemical shifts in random coiling chains are virtually independent of sequence. The one exception to this statement occurs when a residue precedes an *imino* residue such as Pro or Hyp (Christl and Roberts, 1972). In this case, it is evident from the results in Table I that the C^α and C^β chemical shifts are systematically upfield of their corresponding values when the given residue precedes an *amino* acid residue. The known sequence of α1-CB2 (Bornstein, 1967) was used to determine the residues which precede Pro or Hyp, and these residues were assigned using the results in Table I. Spectra of *N*-acetylhomoserine and *N*-acetylhomoserinelactone were used to assign the carbons of the C-terminal residues,[4]

[4] These assignments were confirmed by the reversible changes in the intensity of the Hse resonances accompanying the reaction Hse-OH ⇌ Hse-OH-lactone.

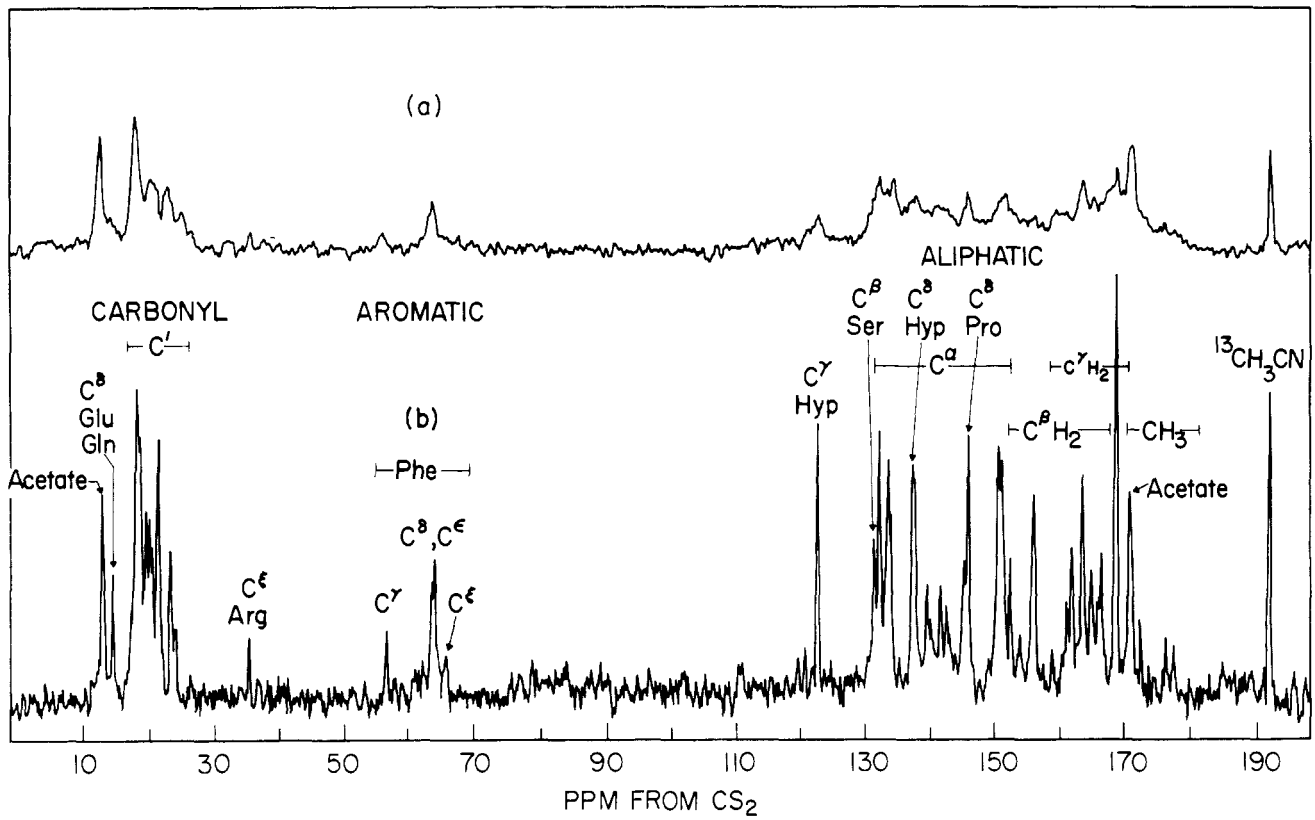

FIGURE 1: Comparison of α1-CB2 spectra obtained at two temperatures using 90°-t-90° pulse sequences: (a) 2°, t = 1.5 sec, 32K scans of the FID accumulated; (b) 30°, t = 4.5 sec, 16K FID accumulated with vertical scale multiplied by two to facilitate comparison with the 2° spectrum. Protein concentration, 25mg/ml in 0.15M AcONa buffer at pH 4.8. Chemical shift scale in ppm from exteranl CS_2.

Table I: Influence of a Pyrrolidine Residue on the C-13 Shifts of the Preceding Residue, R.[a]

Residue R	Carbon	Chemical Shift in Sequence R-Z[b]	Chemical Shift in Sequence R-Pyr[c]
Gly	C^{α}	149.9–150.4	150.6–150.8
Ala	C^{α}	143.5	145.2
Ser	C^{α}	137.1	139.2
Pro	C^{α}	131.6–132.6	134.2
Hyp	C^{α}	133.3	135.3
Ala	C^{β}	176.3	177.1
Ser	C^{β}	131.4	132.1
Pro	C^{β}	162.8–163.7	164.8
Hyp	C^{β}	155.3	156.8
Pro	C^{γ}	168.3	168.3
Hyp	C^{γ}	122.5	122.7
Pro	C^{δ}	145.0–145.7	145.1–145.2
Hyp	C^{δ}	138.0	137.8

[a] Data obtained on the National Bureau of Standards 15.08-MHz spectrometer from spectra of poly(Pro), poly(Hyp), poly(Pro-Gly), poly(Hyp-Gly), poly(Gly-Gly-Pro-Gly), poly(Ala-Pro-Ala), poly(Pro-Pro-Ala), poly(Pro-Ser-Gly), and poly(Ser-Pro-Gly). Chemical shifts are in ppm from external CS_2, uncertainty ±0.2 ppm. [b] Z stands for Gly, Ala, or Ser. [c] Pyr stands for Pro or Hyp.

while the carbons in the remaining residues were assigned using results in the literature. The α1-CB2 random coil assignments are listed in Table II and the aliphatic spectrum calculated using these assignments (Figure 2b) is an excellent simulation of the experimental spectrum (Figure 2a).

The small resonance at 125.1 ppm is assigned to the Hyp C^{γ} carbons in cis X-Hyp peptide bonds on the basis of polypeptide spectra (Torchia and Lyerla, 1974). The intensity of this resonance shows that ≤10% of the X-Hyp bonds are cis, and the strong resonance at 168.2 ppm (C^{γ}-Pro-trans) shows that at least 85% of the Gly-Pro bonds are trans. The C^{γ}-Pro-cis is known to resonate at 170–170.5 ppm (Dorman and Bovey, 1973; Torchia *et al.*, 1974b) and thus has the same chemical shift as one Leu methyl and the acetate methyl. Upon removing the acetate from the solution, (see Experimental Section) an intensity of ≤2 carbons was measured for the resonance centered at 170.4 ppm (C^{γ}-Pro-cis plus one CH_3 of Leu) confirming that ≤15% of the Gly-Pro bonds are cis. The predominance of trans bonds in the coil form of α1-CB2 is in agreement with results obtained for random coiling copolypeptides composed of Gly and Pro or Gly and Hyp but contrasts with the recent report (Kobayashi and Kyogoku, 1973) that *ca.* 50% of the R-Pro peptide bonds are cis in the random coil form of the polytripeptide (Pro-Pro-Gly)$_n$, n = 10,15, dissolved in aqueous solution.[5]

[5] The observation of two separate Pro α-proton resonances of *ca.* equal intensity forms the basis of the proposal of Kobayashi and Kyogoku (1973) that 50% of the R-Pro (R = Gly or Pro) peptide bonds are cis in the polytripeptide. However, 220-MHz proton spectra of the polypeptides listed in Table I show that the α-proton chemical shift of a given residue R is perturbed when the given residue precedes an imino residue (Pro or Hyp). In each case the H^{α}-R shift in the sequence R-Pro (or R-Hyp) is *ca.* 0.2–0.4 ppm downfield of the H^{α}-R chemical shift in sequence R-Z (Z-an *amino* acid). Hence the proposed cis assignments of Kobayashi and Kyogoku (1973) must be confirmed by additional evidence (^{13}C spectra, solvent induced changes in relative intensity of the resonances) before we can accept them.

Table II: Random Coil Chemical Shifts,[a] Assignments, Spin-Lattice Relaxation Times,[b] and Effective Correlation Times.[c]

Chemical Shift	Relative Intensity	Carbon–Residue–Position in Chain	T_1	τ_{eff}
177.1	1.0	C^{β}–Ala–(14)	0.3	0.05
175.9	1.0	C^{β}–Ala–(32)	0.3	0.05
172.1	1.0	C^{δ}–Leu–(8)	0.3	0.05
170.3–170.6	2.0	CH_3 in AcONa Buffer		
	1.0	C^{δ}–Leu(8)		
168.1–168.4	6.5	C^{γ}–Pro–(2,5,11,17,23,35)	0.15	0.16
	1.0	C^{γ}–Leu–(8)		
	1.0	C^{γ}–Arg–(6)		
165.5–166.2	2.0	C^{β}–Gln–(18,21)	0.09	0.26
	2.0	C^{β}–Glu–(26,29)		
164.5–164.9	2.0	C^{β}–Pro–(11,23)	0.09	0.26
	1.0	C^{β}–Arg–(6)		
	0.4	C^{β}–Hse-OH-lactone–(36)		
163.3	4.5	C^{β}–Pro–(2,5,17,35)	0.135	0.17
161.4–161.6	2.0	C^{γ}–Glu–(26,29)	0.15	0.16
	1.0	C^{γ}–Gln–(18)		
160.7	1.0	C^{γ}–Gln–(21)		
158.7	0.6	C^{β}–Hse-OH–(36)		
155.3–155.7	5.5	C^{β}–Hyp–(9,12,15,24,27,30)	0.07	0.34
	1.0	C^{β}–Phe–(20)		
153.5	1.0	C^{β}–Leu–(8)	0.07	0.34
151.9	1.0	C^{δ}–Arg–(6)	0.17	0.14
	1.0	C^{α}–Gly–(1)		
150.6–150.9	6.0	C^{α}–Gly–(4,10,16,22,34)	0.065	0.36
150.0–150.3	5.0	C^{α}–Gly–(7,13,19,25,28,31)		
145.0–145.7	6.5	C^{δ}–Pro–(2,5,11,17,23,35)	0.085	0.28
	1.0	C^{α}–Ala–(14)		
	0.4	C^{α}–Hse-OH-lactone–(36)		
142.3–142.7	1.0	C^{α}–Ala–(32)	0.12	0.39
	1.0	C^{α}–Leu–(8)		
141.3	2.0	C^{α}–Glu–(26,29)	0.11	0.43
139.3–139.9	2.0	C^{α}–Gln–(18,21)	0.12	0.39
	1.0	C^{α}–Arg–(6)		
	0.6	C^{α}–Hse-OH–(36)		
136.9–137.5	5.5	C^{δ}–Hyp–(9,12,15,24,27,30)	0.07	0.34
	2.0	C^{α}–Ser–(3,33)		
	1.0	C^{α}–Phe–(20)		
132.8–133.8	5.5	C^{α}–Hyp–(9,12,15,24,27,30)	0.105	0.45
	2.0	C^{α}–Pro–(11,23)		
	0.6	C^{γ}–Hse-OH–(36)		
132.0–132.1	4.5	C^{α}–Pro–(2,5,17,35)	0.15	0.32
131.5	2.0	C^{β}–Ser–(3,33)	0.14	0.17
125.5	0.4	C^{γ}–Hse-OH-lactone–(36)		
125.1	0.5	C^{γ}–Hyp–(9,12,15,24,27,30)		
122.5–122.8	5.0	C^{γ}–Hyp–(9,12,15,24,27,30)	0.135	0.35
65.5	1.0	C^{ζ}–Phe–(20)	0.17	0.27
63.9	2.0	C^{ϵ}–Phe–(20)	0.17	0.27
63.5	2.0	C^{δ}–Phe–(20)		
56.7	1.0	C^{γ}–Phe–(20)		
32.4	1.0	C^{ζ}–Arg–(6)		
18.5–24.3	36.0	C′–All residues	1.4	
14.7	4.0	C^{δ}–Gln,Glu		
13.2		CO in AcNa buffer		

[a] In ppm from external CS_2. [b] In sec. [c] In nsec.

In contrast with the aromatic and aliphatic resonances, few of the C′ resonances can be assigned. The available polypeptide data suggest that the α1-CB2 resonances at 23.7–24.3 ppm are due to the Gly residues which precede Pro residues, and that the large resonance centered at 18.7 ppm is due primarily to Pro and Hyp residues. However, even these limited assignments are tentative, since the effect of sequence on the C′ chemical shifts is now known, due to the difficulty of assigning C′ resonances in copolypeptides.

Random Coil T_1 Values and Correlation Times. The spin-lattice relaxation times (T_1) of the α1-CB2 carbons in the random coil were obtained from inversion-recovery Fourier transform spectra (Figure 3) using the procedure outlined in the Experimental Section. The T_1 values so obtained (Table II) have estimated uncertainties of 10–25%, with the larger error associated with resonances of low intensity. Due to their large T_1 values, only three inversion-recovery spectra were obtained for the C′ resonances, and hence the uncertainties in the C′ T_1 values is *ca.* 25%.

Utilizing the result (Table II) that the C′ T_1 values are less than 1.5 sec, proton coupled and decoupled 90°–t–90° spectra were obtained using t = 4.5 sec (ensuring negligible saturation of the resonances). These experiments showed that the C′ NOE was maximal, within experimental error, since the area under the C′ resonances was found to decrease by a factor of 2.8 ± 0.3 when the C′ spectrum was obtained without decoupling. A maximal NOE was also deduced for the aliphatic carbons since the ratio of areas of aliphatic to C′ resonances (measured with proton decoupling and t = 4.5 sec) was found to be 2.7 ± 0.3, in agreement with the theoretical value (2.61) calculated from the amino acid composition. In line with these results, maximal NOE values have been reported (Torchia and Lyerla, 1974) for random coiling copolypeptides of Pro and Gly.

The fact that the NOE is maximal has two important consequences. First, the carbon relaxation times are determined solely by the ^{13}C–^{1}H dipole-dipole interaction, and second, the motional narrowing condition is valid, *i.e.*, $(\omega_H + \omega_C)^2\tau_r^2 \ll 1$ where τ_r is a rotational correlation time and ω_C and ω_H are the respective Larmor precession frequencies of the ^{13}C and ^{1}H nuclei. Under these conditions, an effective rotational correlation time (Woessner, 1962), τ_{eff}, for

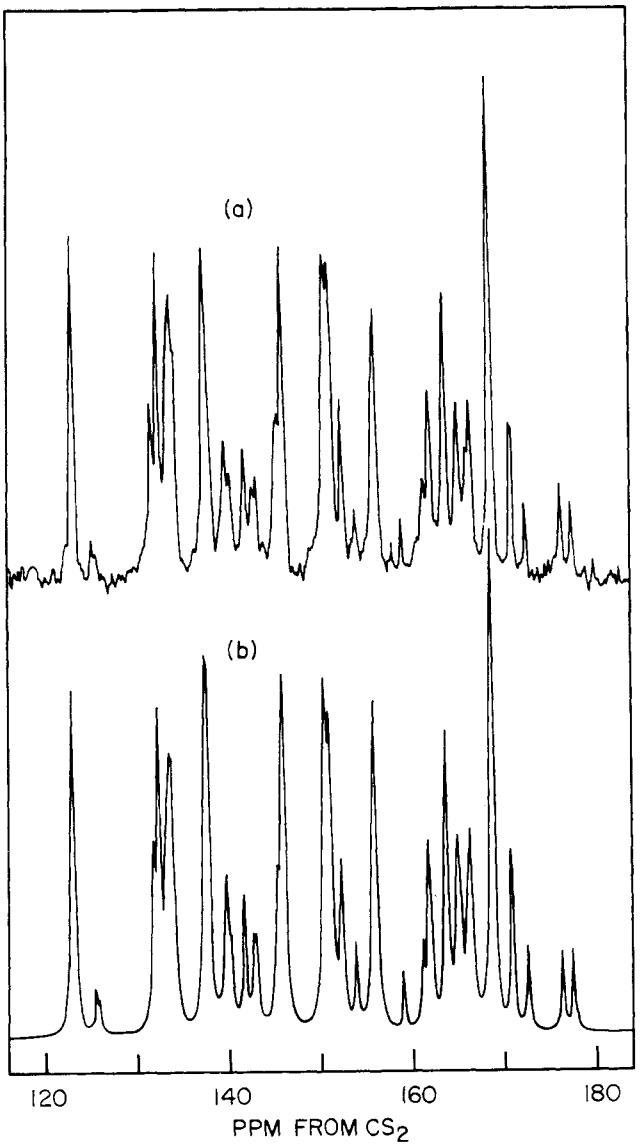

FIGURE 2: Comparison of experimental and calculated random coil spectra in the aliphatic region: (a) experimental spectrum, 30° 64K FID accumulated, protein concentration 25 mg/ml in 0.15 M AcONa buffer at pH 4.8; (b) computer simulation. Chemical shifts in ppm from external CS_2.

the vector connecting directly bonded C and H atoms is given by (Allerhand *et al.*, 1971)

$$\tau_{eff} = r_{CH}^{6}/KT_1N_H \quad (1)$$

where r_{CH} is the internuclear distance (1.09 Å), T_1 is the spin-lattice relaxation time, N_H is the number of bonded hydrogens, and K is a constant equal to 3.56×10^{10} Å^6 sec^{-2}.

Some comment regarding the physical meaning of τ_{eff} is in order. The simplest model for C^{α}–H^{α} rotational motion assumes that backbone segmental motion results in isotropic rotational diffusion of the C^{α}–H^{α} internuclear vector. In this case, $\tau_{eff} = 1/(6R)$, where R is the rotational diffusion constant characterizing the C^{α}–H^{α} reorientation (Abragam, 1961). While available evidence (Torchia and Lyerla, 1974) suggests that C^{α}–H^{α} reorientation in random coil copolypeptides is approximately isotropic, the side chain C–H reorientation is manifestly anisotropic due to rotation about side chain single bonds. Two or more correlation times are required to characterize anisotropic reorientation (Woessner, 1962; Woessner *et al.*, 1968), and the τ_{eff} value calculated using eq 1 is a weighted average of these correlation times, *i.e.*, $\tau_{eff} = \Sigma c_i\tau_i$, where c_i are orientation dependent coefficients. The τ_i are functions of the various molecular rotation rates and quantitative values of these rates can be obtained from the τ_{eff} value only if a detailed model of the (complex) molecular motion is assumed (Woessner *et al.*, 1968; Wallach, 1967; Levine *et al.*, 1974).

Although precise interpretation of τ_{eff} is difficult when

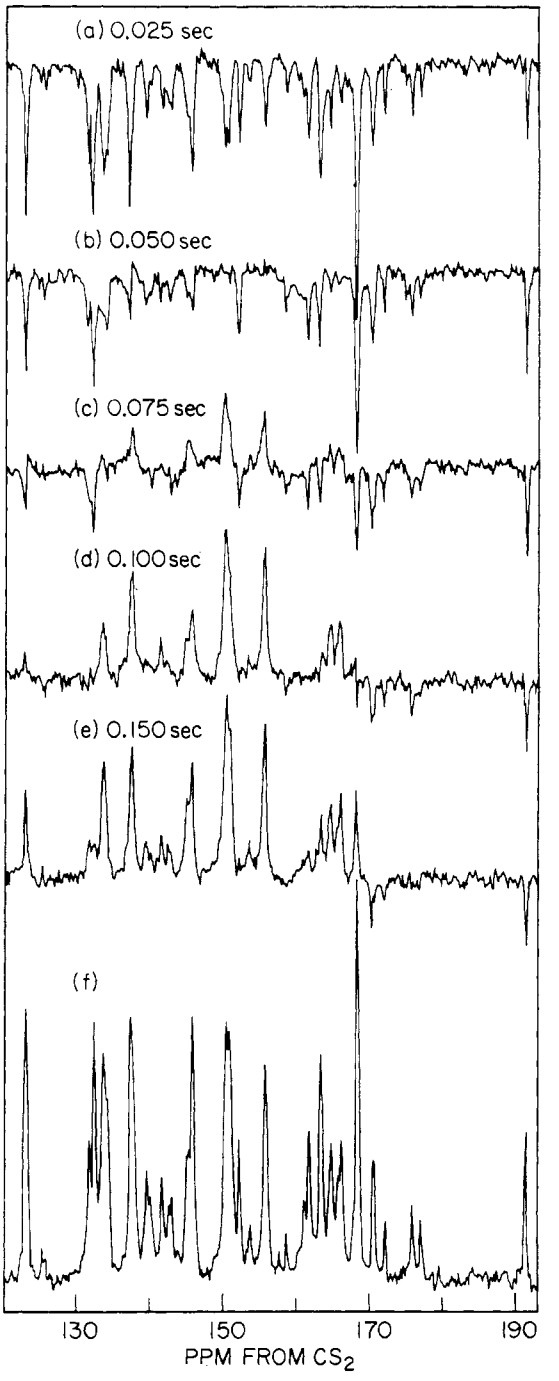

FIGURE 3: Partially relaxed random coil spectra of α1-CB2 in the aliphatic region obtained using 180°–t–90° pulse sequences with (a) t = 0.025 sec; (b) t = 0.050 sec; (c) t = 0.075 sec; (d) t = 0.10 sec; (e) t = 0.15 sec. In each case 64K FID were accumulated with a 0.75-sec delay between the 90 and 180° pulses. For the 90°–t–90° spectrum, (f) 96K FID were accumulated with t = 0.75 sec and the vertical amplitude has been multiplied by two-thirds to facilitate comparison with the partially relaxed spectra. Protein concentration, temperature, solvent, and chemical shift scale are as in Figure 2.

molecular motion is complex, the τ_{eff} values in Table II provide an approximate measure of the mobility of various α carbons in the α1-CB2 random coil. For instance, of the 12 pyrrolidine C^{α} carbons in α1-CB2, 4.5 are Pro C^{α} which resonate at 132.1 ppm while the remaining 7.5 pyrrolidine C^{α} resonate at 132.8–133.8 ppm. The distribution of the Pro C^{α}, which resonate at 132.1 ppm and have an average τ_{eff} = 0.32 nsec, is such that three of these C^{α} are in residues whose position is within five residues of the chain termini, whereas the higher field pyrrolidine α carbons have τ_{eff} = 0.45 nsec and are in residues which are located at least seven residues from the chain ends. With the exception of the C^{α} of Hse the various C^{α} which resonate in the 139–143-ppm range are at least five residues from the chain ends and have an average τ_{eff} value (*ca.* 0.4 nsec) closer to that of the higher field pyrrolidine C^{α}. The N-terminal Gly residue has the smallest C^{α} τ_{eff} value (*ca.* 0.14 nsec) while the remaining Gly residues, distributed uniformly along the chain, have an average τ_{eff} value of 0.36 nsec. Hence, the position of a residue in the α1-CB2 chain, rather than the residue type, determines C^{α} τ_{eff} values. This result is consistent with the idea that cooperative segmental motion reorients the C–H vectors in the backbone. Clearly, the motion of residues at or near chain termini requires cooperative movement of fewer atoms, resulting in larger T_1's (smaller τ_{eff} values) for those ^{13}C signals composed largely of near-terminal α-carbon resonances.

In the residues having linear side groups, C^{β}, C^{γ}, and CH_3 τ_{eff} values are smaller than their corresponding C^{α} correlation times due to local motion in the side chains. Methyl moieties have the smallest τ_{eff} values since complete axial reorientation of the methyl group results from random rotational jumps among its three equivalent sites. Even the limited motion in the Pro ring is reflected in the fact that τ_{eff} of the Pro C^{β} which resonate at 163.3 ppm is one-half the value found for the Pro C^{α} in the same residues (which resonate at 132.1 ppm). The Hyp C^{α} and C^{γ} τ_{eff} values differ by less than 35% indicating that the Hyp ring is less mobile than the Pro, in agreement with results obtained for the synthetic copolypeptides (Torchia and Lyerla, 1974). In summary, the τ_{eff} values provide a reasonable picture of motion in the random coil,[6] and it is now of interest to compare the coil τ_{eff} values with the correlation times found for the helix.

Assignments and Line Widths in the 2° Spectrum. Assignment of resonances in the aliphatic portion of the 2° spectrum (Figure 4e) is complicated by the presence of random coil conformations at 2°. The thermodynamic parameters of Piez and Sherman (1970b) predict that *ca.* 3% of α1-CB2 is in the random coil state under the conditions used in the present study, *i.e.*, 2°, 25 mg/ml, and the large activation energy (18 kcal/mol) of the helix–coil transition means that the two conformations have separate spectra. Also, as noted in the Experimental Section, the sample contained (*ca.* 1% by weight) the 15 residue fragment α1-CB1. This peptide is in a random coil state at 2° since it is not composed of Gly-X-Y triplets. Although the fraction of random coil is small, it contributes measurably to the 2° spectrum because the peak height of a single carbon in the coil is 5–10 times larger than in the helix, due to the smaller line widths and larger NOE values of the coil resonances. The random coil component of the 2° spectrum (Figure 4a) was calculated using the chemical shifts and line widths given in Table II.[7]

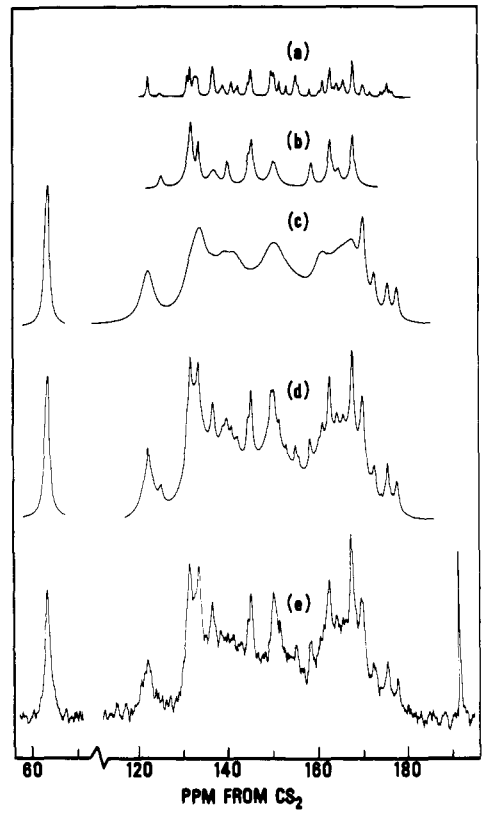

FIGURE 4: Comparison of α1-CB2 aromatic and aliphatic low temperature (2°), spectra: (a) calculated spectrum of α1-CB2 and α1-CB1 random coil; (b) calculated spectrum of near terminal helix residues; (c) calculated spectrum of residues in rigid portion of the helix; (d) sum of calculated spectra (a), (b), (c); (e) experimental spectrum, 2°, 400K FID accumulated, concentration 25 mg/ml in 0.15 M AcONa buffer at pH 4.8. Chemical shifts in ppm from external CS_2.

Coil resonances are narrow due to the rapid reorientation of the flexible polypeptide backbone. Backbone motion is possible for residues near the ends of the α1-CB2 helix. A schematic representation of the terminal regions in an α1-CB2 triple helix, having a complete set of interchain hydrogen bonds, is given in Figure 5. As seen, the staggered arrangement of the chains permits rotation about backbone bonds for the Hse residues and certain Gly and Pro residues in the two terminal triplets. Since the terminal hydrogen bonds can be broken independently of each other they are expected to be broken some fraction of the time, allowing backbone mobility to additional Gly and Pro residues as well as Ser residues in the terminal regions of the trimer. Hence, two classes of line widths were used to calculate the spectrum (Figure 4b) of the mobile residues in the terminal regions of the trimer. Those residues having mobility with a

[6] The uncertainties in the absolute values of the correlation times (10–25%) arise from a variety of sources. Certain sources of error such as temporal fluctuations in amplifier gain and imperfections in the 180° pulse introduce similar errors in the measured T_1 values of all resonances. Hence, *differences* in T_1 values are largely unaffected by these sources of error and we believe the differences in τ_{eff} values discussed in the text are outside the range of experimental error. Relative T_1 values are also accurately obtained from measurements of the times at which signal intensities null in partially relaxed spectra. Relative τ_{eff} values obtained from such t_{null} experiments are in agreement with those in Table II.

[7] Since the measured random coil line widths are essentially due to field drift, digital filtering, and chemical shift inequivalence, the fact that the natural line widths are 1–2 Hz larger at 2° was neglected.

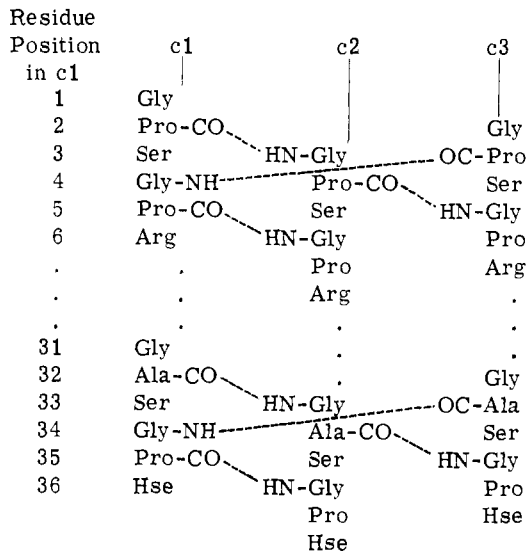

FIGURE 5: Schematic representation of the interchain hydrogen bonds (dashed lines) in the terminal regions of the α1-CB2 helix. The three covalently linked chains are labeled c1, c2, and c3.

Table III: Assignments and Nmr Parameters[a] for Mobile Residues in the Terminal Regions of the α1-CB2 Trimer.

Chemical Shift[b]	Assignment Carbon–Residue–Position	Residues/Trimer	T_1[c]	Line Width[d]	NOE
168.1	C^{γ}–Pro–(2,35)	3	0.05	40	1.35
168.1	C^{γ}–Pro–(2,35)	3	0.09	12	1.5
164.9	C^{β}–Hse-OH-lactone–(36)	1	0.06	15	1.5
163.1	C^{β}–Pro–(2,35)	3	0.06	13	1.5
163.1	C^{β}–Pro–(2,35)	3	0.04	50	1.35
158.8	C^{β}–Hse-OH–(36)	2	0.06	15	1.5
150.5	C^{α}–Gly–(1)	2	0.05	25	1.5
150.5	C^{α}–Gly–(1,34)	3	0.04	40	1.35
145.7	C^{δ}–Pro–(2,35)	3	0.06	13	1.5
145.6	C^{δ}–Pro–(2,35)	3	0.04	62	1.35
144.9	C^{α}–Hse-OH-lactone–(36)	1	0.08	10	1.5
140.3	C^{α}–Hse-OH–(36)	2	0.08	15	1.5
137.2	C^{α}–Ser–(3,33)	4	0.05	36	1.35
133.9	C^{γ}–Hse-OH–(36)	2	0.15	10	1.5
132.2	C^{α}–Pro–(2,35)	3	0.05	27	1.35
132.2	C^{α}–Pro–(2,35)	3	0.06	14	1.5
131.7	C^{β}–Ser–(3,33)	4	0.04	40	1.35
125.5	C^{γ}–Hse-OH-lactone–(36)	1	0.10	15	1.5

[a] Obtained from computer simulation. [b] In ppm from external CS_2. [c] In sec. [d] In Hz.

complete set of hydrogen bonds have line widths less than 15 Hz (Table III) while the remaining residues—having backbone mobility once a terminal hydrogen bond is broken—have line widths greater than 25 Hz. The variability of line widths for residues in the same class reflects the differences in number of protons bonded to a given carbon and the greater mobility expected for side chain carbons as compared with C^{α} carbons. The line widths listed in Table III

Table IV: Chemical Shifts,[a] Assignments, T_1,[b] Line Width,[c] and NOE Values of α1-CB2 Carbons in the Triple Helix.

Chemical Shift	Carbon–Residue	T_1[d]	Line Width[e]	NOE[f]
178.0	C^{β}–Ala	0.1 (0.1)[f]	16[d] (22)[f,g]	1.5 (1.2)[f]
175.7	C^{β}–Ala	0.1 (0.1)	16[d] (22)	1.5 (1.2)
172.9	C^{δ}–Leu	0.1 (0.1)	16[d] (16)	1.5 (1.2)
170.6	C^{δ}–Leu		16 (16)	1.5 (1.2)
170.3	CH_3 in AcONa		18	
168.2	C^{γ}–Pro,Leu,Arg	0.045	80,50,80	1.35
165.7–166.2	C^{δ}–Gln,Glu	0.045	90	1.35
164.5–164.9	C^{δ}–Pro,Arg	0.045	90	1.35
163.3	C^{β}–Pro	0.045	100	1.35
160.7–161.6	C^{γ}–Gln,Glu	0.04	80	1.35
155.3–155.7	C^{β}–Hyp,Phe	0.04	150,100	1.35
153.1	C^{β}–Leu		100	1.35
151.9	C^{δ}–Arg		100	1.35
150.1–150.9	C^{α}–Gly	0.025	90	1.35
145–146	C^{δ}–Pro,C^{α}–Ala	0.04	125,54	1.35
139–143	C^{α}–Gln,Arg,Glu, Leu,Ala	0.04	54	1.35
137–137.5	C^{δ}–Hyp	0.03	150	1.35
137–137.5	C^{α}–Ser,Phe	0.04	54	1.35
132.8–133.8	C^{α}–Hyp,Pro	0.04	54	1.35
131.5–132.1	C^{α}–Pro,C^{δ}–Ser	0.04	54,60	1.35
122.7	C^{γ}–Hyp	0.04	50	1.35
65.5	C^{δ}–Phe		90	1.35
63.5–63.9	C^{δ},C^{ϵ}–Phe	0.085	15[d]	1.9
32.4	C^{δ}–Arg		5	
18–25	C′–All residues	0.6		1.35
14	C^{δ}–Gln,Glu			

[a] In ppm from external CS_2. [b] In sec. [c] In Hz. [d] Uncertainty *ca.* ±30%. [e] Obtained from computer simulation, unless noted otherwise, uncertainty *ca.* ±40%. Listed line widths include 3–5 Hz broadening due to magnetic field drift and digital filtering. [f] Values in parentheses were calculated as described in the text. [g] Drift and digital broadening not included.

yielded a calculated spectrum, which, when added to the calculated random coil spectrum, provided the best representation of the narrow resonances in the 2° spectrum.

It was not possible to calculate the broad component of the 2° spectrum—resonances due to carbons in the interior of the trimer—without making some assumption regarding the chemical shifts of the poorly resolved helix resonances. The simplest assumption was made, *i.e.*, that the chemical shifts of carbons in the trimer were essentially the same as those in the random coil. The broad component was then calculated and added to the calculated narrow component spectra, varying the line widths of the broad resonances until the sum of the calculated components (Figure 4d) matched the experimental spectrum (Figure 4e). The chemical shifts and line widths used to calculate the spectrum of the residues in the rigid portion of the trimer (Figure 4c) are summarized in Table IV.

It is not claimed that the agreement between the calculated (Figure 4d) and experimental spectrum (Figure 4e)

precisely determines the parameters listed in Tables III and IV. Clearly there are too many parameters which can be adjusted in a compensating fashion for this to be the case. However, the numerous attempts to simulate the experimental spectrum, using various combinations of component spectra, did demonstrate that a satisfactory simulation resulted only when contributions were included from all components, *i.e.*, α1-CB2 plus α1-CB1 random coil, flexible terminal residues in the trimer, and rigid residues in the interior of the trimer. This result is gratifying since presence of α1-CB2 random coil is in accord with results of the optical data and the flexibility of the near-terminal residues confirms the conclusion inferred from optical rotation data, that the terminal regions of the trimer are not helical.

Since the line widths of the residues in the rigid portion of the trimer (Table IV) are to be used to estimate helix correlation times, a measure of the uncertainty in these parameters is needed. Most of the line widths in Table IV can be reduced by a factor of 2–3 and the calculated spectrum will satisfactorily match the experimental spectrum, provided that the reduction in line widths is compensated by an increase in the inequivalence in the chemical shifts. However, due to the regular backbone structure of the helix, it is reasonable to assume that the C^{α} carbons of a given type of residue exhibit no greater chemical shift inequivalence in the helix than in the coil. This statement also applies to side chain chemical shifts, since the side chains are on the surface of the helix in contact with solvent, as is the case in random coil. Hence, we believe one can justifiably constrain the inequivalence in the helix shifts to be no greater than found in the coil, and subject to this constraint, the 40% uncertainties in line widths (Table IV) indicate the amount that the listed line widths can be varied, and yet yield simulations whose quality is about equal to that shown in Figure 4d.

Finally, it is worth noting that while the chemical shifts used to simulate the helix and coil spectra are essentially the same, it is probable that carbons in the two states have chemical shift differences which are masked by the great width of helix resonances. ^{13}C studies of the α helix–random coil transition of homopolypeptides show that residues in the two states have chemical shift differences of *ca.* 0–2 ppm (Lyerla *et al.*, 1973; Saito and Smith, 1973). Unfortunately, similar studies have not yet been made of the triple helix–random coil transition of polytripeptides. Since the α helix–random coil transition involves considerably larger changes in average ϕ, ψ angles (IUPAC–IUB Commission, 1970) than the triple helix–random coil transition, the available data suggest that the differences in the chemical shifts in the α1-CB2 helix and coil states are small compared with the line widths of the helix.

Recently it has been suggested that the $(Pro\text{-}Hyp\text{-}Gly)_{10}$ triple helix contains cis Gly–Pro peptide bonds (Berg *et al.*, 1974). Since the Pro C^{γ} cis resonances (if present) and the downfield Leu C^{δ} resonance in the α1-CB2 trimer are masked by the strong acetate methyl resonance at 170 ppm, a spectrum of α1-CB2, in 0.15 M NaCl (pH 4.8) at 2° was obtained. The resulting spectrum was found to have an intensity less than two carbons at *ca.* 170 ppm. Since the Leu C^{δ} resonance accounts for one carbon, no more than 15% of the Gly–Pro bonds are cis in the α1-CB2 trimer.

NOE and T_1 Values at 2°. A comparison of areas of the C′ resonances in the helix, with and without proton decoupling, yielded a C′ NOE of 1.4 ± 0.3. This same average NOE was deduced for the aliphatic carbons, since the measured ratio of areas of aliphatic and C′ resonances was equal to the theoretical value, known from the amino acid composition. The helix NOE values were also obtained by comparing areas of helix C′ and aliphatic resonances with the respective areas measured in random coil spectra. This method yielded NOE values of 1.4 ± 0.3 for both C′ and aliphatic carbons in the helix. Although the average NOE for

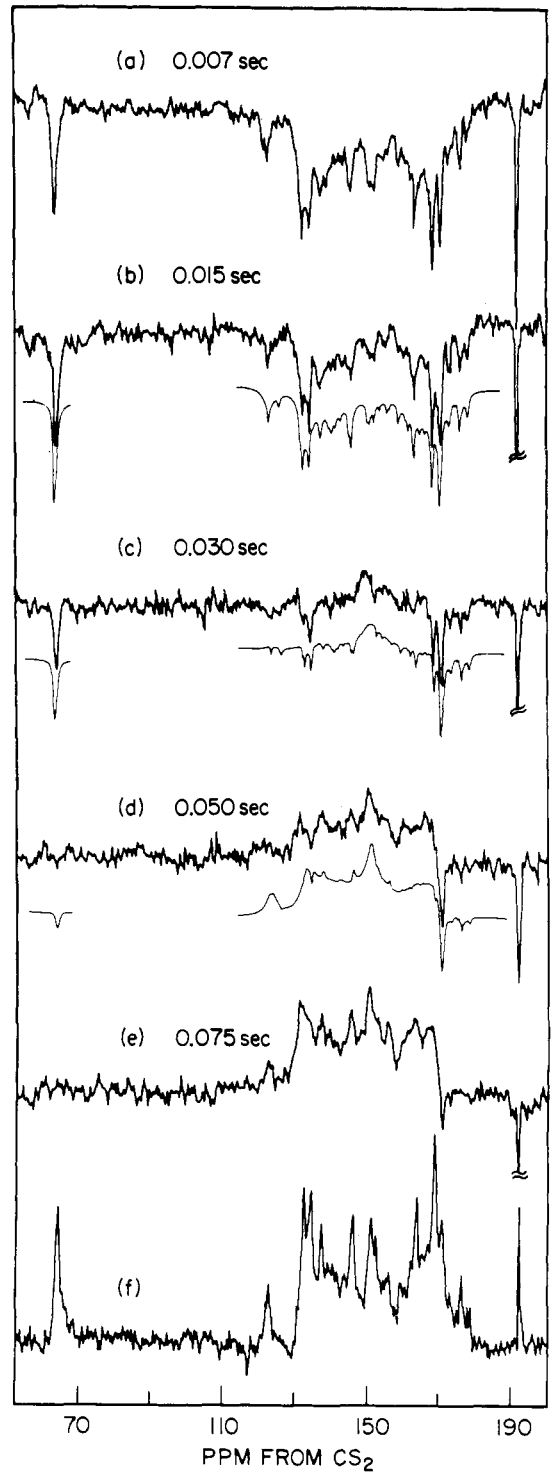

FIGURE 6: Low temperature (2°) partially relaxed spectra of α1-CB2 in the aromatic and aliphatic regions obtained using 180°–t–90° pulse sequences with (a) t = 0.007 sec; (b) t = 0.015 sec; (c) t = 0.030 sec; (d) t = 0.050 sec; (e) t = 0.075 sec (a 0.4-sec delay was used between the 90 and 180° pulses); (f) a 90°–t–90° spectrum with t = 0.4 sec. In each case 192K FID were accumulated and protein concentration, temperature, solvent, and chemical shift scale are as in Figure 4. Calculated spectra are shown as the noiseless traces in (b), (c), and (d).

the aliphatic carbons is 1.4, the NOE of the flexible carbons, in the terminal triplets, was found from the simulations to be larger than for the rigid carbons. This result was expected since the NOE generally shows a rapid monotonic increase with increased molecular mobility when the NOE is in the range 1.4–2.6. An NOE value of 1.5 was used for the flexible terminal carbons in calculating the simulation (Figure 4b).

The helix spin-lattice relaxation times, T_1, listed in Tables III and IV were obtained from inversion-recovery spectra (Vold *et al.*, 1968) (180°-t-90° pulse sequences) in the following manner. Initial estimates of the T_1 values were made by inspection of the inversion-recovery spectra, and then these T_1 values were used to calculate simulations of spectra in Figure 6. The T_1 values were then adjusted, by trial and error, until a satisfactory simulation was obtained. A comparison of the calculated (noiseless) and experimental partially relaxed spectra is provided in Figure 6b–d.

It is seen in Tables III and IV that the broad resonances have significantly shorter T_1 values than the narrow lines. Hence, the intensities of the broad lines null at $t \approx 0.03$ sec whereas the sharp lines are near null when $t = 0.05$–0.075 sec. For this reason, the spectra in Figures 6d and e have a broad appearance compared to the spectrum in Figure 6b.

In summary, T_1 and NOE values are significantly smaller in the helix than in the coil, while the helix line widths are much larger. All these results indicate that molecular motion is much slower in the helical state. However, before quantitative information on helical motion can be extracted from the nmr data, a model for the motion of the helix must be developed.

A Model for the Motion of the Helix. It is supposed that α1-CB2 behaves, in solution, like a rigid (prolate) ellipsoid of revolution undergoing rotational diffusion. The primary reason for choosing an ellipsoid model for the helix is that expressions are available which relate the T_1, line width, and NOE values to the rotational diffusion constants of the ellipsoid. Also, a prolate ellipsoid appears to approximate the shape of the α1-CB2 helix as well as any simple solid, since the different sizes of the amino acid side chains result in a helix having nonuniform cross section.

The dimensions of the ellipsoid of revolution, a (the semimajor axis) and b (the semiminor axis), were calculated for two models of the triple helix in solution. In the first model the helix was assumed to be unhydrated. Hence, the product of its mass (9936 daltons) with its partial specific volume ($\bar{v}$ = 0.69 cm^3/g) yields a helical volume V_A = 1.14×10^4 Å^3. From V_A and the total length of the helix, l = 113 Å, an average diameter of 11.4 Å is obtained (Piez and Sherman, 1970a). The dimensions of the ellipsoid of revolution (Table V) corresponding to the hydrated helix were calculated by setting $\rho \equiv b/a = d/l$ (*i.e.*, $\rho = 1/10$) and requiring that the volume of the ellipsoid ($4\pi ab^2/3$) was equal to V_A.

In the second model the presence of bound water was assumed to increase the dimensions of the anhydrous helix by 3 Å, *i.e.*, l = 116 Å, d = 14.4 Å. This value of d corresponds closely to the separation of the collagen helices in hydrated fibers. The dimensions of the corresponding ellipsoid (Table V) were calculated in the manner described for the anhydrous model.

Using the dimensions thus obtained, the two rotational diffusion constants which describe the reorientation of the ellipsoid can be calculated using the theory of Perrin (1936). Following Woessner (1962), these diffusion constants are designated R_1 and R_2 and they are, respectively, the diffusion constants for reorientation about the long axis of the ellipsoid and an axis perpendicular to the long axis. For prolate ellipsoids having $\rho^2 \ll 1$ ($\rho = b/a$) Perrin's expressions for R_2 and R_1 are

$$R_2 = (3kT/16\pi\eta a^3)[2 \ln (2/\rho) - 1]$$
$$R_1 = \sigma R_2 , \ \sigma^{-1} = \rho^2[2 \ln (2/\rho) - 1] \quad (2)$$

In these equations, k is Boltzmann's constant, T is the Kelvin temperature, and η is the viscosity of the solvent. Using the dimensions of the anhydrous and hydrated ellipsoid models of the helix, values of R_2 and σ were calculated (Table V). As expected, $\sigma \gg 1$, since both ellipsoid models have rod-like shapes. The error in the calculated value of R_2 may be large if the solvent viscosity (used in the calculation) poorly approximates the local viscosity between solvent and solute. The calculated value of σ is not subject to this uncertainty.

Table V: Dimensions[a] and Rotational Diffusion Constants[b] of α1-CB2 Ellipsoid Models.

	Anhydrous Model	Hydrated Model
Length of major axis	130	132
Length of minor axis	13	16.4
σ (= R_1/R_2)	20	14
R_2 (theory)	2.5×10^6	2.2×10^6
R_2 (experiment)[c,d]	1.0×10^6	1.3×10^6

[a] In Å. [b] In sec^{-1}. [c] Calculated using eq 2 with T = 275°K, η = 1.67 cP. [d] Estimated uncertainty, ±40%.

The spectral densities, $J(\omega)$, needed to calculate nuclear spin relaxation times in rigid ellipsoids have been obtained (Woessner, 1962) using the rotational diffusion theory of Perrin (1936). Combining the equations for $J(\omega)$ with Solomon's (1955) dipole relaxation theory yields the following expression for the T_1 of a carbon bonded to a single hydrogen atom[8]

$$1/T_1 = 0.1K r_{CH}^{-6}[J(\omega_H - \omega_C) + 3J(\omega_C) + 6J(\omega_H + \omega_C)] \quad (3)$$

where the spectral densities

$$J(\omega) = A\tau_A/(1 + \omega^2\tau_A^2) + B\tau_B/(1 + \omega^2\tau_B^2) + C\tau_C/(1 + \omega^2\tau_C^2)$$

with $A = (3c^2 - 1)^2/4$, $\tau_A = (6R_2)^{-1}$; $B = 3c^2(1 - c^2)$, $\tau_B = (R_2(\sigma + 5))^{-1}$; $C = 3(c^2 - 1)^2/4$, $\tau_C = (R_2(4\sigma + 2))^{-1}$; and $c = \cos^2\theta$.

In these expressions the constants K, r_{CH}, ω_H, and ω_C are the constants defined earlier in the discussion of eq 1 and θ is the angle between the internuclear C–H vector and the long axis of the ellipsoid. Although the expression for T_1 is lengthy, it does show that the relaxation time depends on only three parameters, R_2, σ, and $\cos^2\theta$. Similar expres-

[8] It should be noted that when the motional narrowing condition applies, eq 3 reduces to eq 1 with $\tau_{eff} = A\tau_A + B\tau_B + C\tau_C$. This result explicitly expresses the fact that when anisotropy is present, τ_{eff} depends upon the orientation of the C–H vector with respect to the rotational axes.

sions can be written for the line width and the NOE, and plots of the nmr parameters as functions of R_2 and θ, with σ held constant, illustrate the results of the theory. Such plots are shown in Figure 7 and were calculated assuming $\sigma = 14$ (the value found for the ellipsoid model of the hydrated helix) for $\theta = 0$, 30, 60, and 90°.

It is of interest to first consider the $\theta = 0°$ curves, since in this case the C–H vector is parallel to the long axis and is not reoriented by rotation about this axis. Hence, when $\theta = 0°$ the calculated curves correspond to isotropic reorientation of the C–H vectors, characterized by a single correlation time $\tau_A = 1/(6R_2)$ *i.e.*, $B = C = 0$ in eq 5. When $\theta > 0°$, B and C are greater than zero so that the terms involving the smaller correlation times τ_B ($\approx\tau_A/3$) and τ_C ($\approx\tau_A/10$) also contribute to $J(\omega)$. The shifts and shape changes of the curves in Figure 7 as θ changes reflect the dependence of the coefficients A, B, and C on θ.

It is clear that the curves in Figure 7 can provide a reliable estimate of R_2 only if the values of $\theta_H{}^\alpha$, the angles between the C^α–H^α internuclear vectors and the helix symmetry axis, are known. The values of these angles have not yet been determined for the α1-CB2 helix. However, the structure of the poly(Gly-Pro-Pro) triple helix in the solid state has been determined by X-rays (Yonath and Traub, 1969; Traub and Piez, 1971) and this structure is assumed to approximate that of the α1-CB2 helix in solution. Using the poly(Gly-Pro-Pro) atomic coordinates the desired angles were calculated using the procedure outlined in the Experimental Section and yielded the following results for the Gly-X-Y residues in the α1-CB2 triplets: $\theta_H{}^{\alpha 2}$ (Gly) = 60°, $\theta_H{}^{\alpha 1}$ (Gly) = 120°, $\theta_H{}^\alpha$ (X) = 105° and $\theta_H{}^\alpha$ (Y) = 90°. Although the Gly C^α is bonded to two hydrogens the fact that $\cos^2$ (120°) = $\cos^2$ (60°) means that the $\theta = 60°$ curves in Figure 7 can be used to determine τ_A from the Gly relaxation data provided that the measured values of the Gly T_1 and line width are multiplied respectively by 2 and 0.5. Since $2T_1$ for the Gly C^α is 0.045 sec, this corresponds to two values of τ_A (6 or 170 nsec). However, the small value of the Gly C^α NOE 1.35 ± 0.3 rules out the smaller value. In concert with this result the value of one-half of the Gly C^α line width (45 Hz) corresponds to τ_A = 110 nsec. Combining the T_1 and line width data for the three types of residues in the triplet yields an average τ_A of 130 nsec for the hydrated ellipsoid and τ_A = 170 nsec for the ellipsoid model assuming no bound water. The corresponding values of R_2 for the two models obtained from these τ_A values ($R_2 = (6\tau_A)^{-1}$) are compared (Table V) with the theoretical values of R_2. The theoretical values of R_2 do not differ greatly in the two models since R_2 is a sensitive function of *a*, but not *b*, for rod-like ellipsoids of revolution. For both models there is reasonable agreement between the theoretical and experimental values of R_2, thus indicating that in solution the α1-CB2 helix behaves as a rigid rod of dimensions 11.5–14.5 Å × 110–120 Å. The better agreement between theory and experimental values of R_2 in the case of the hydrated model ($\sigma = 14$) is of doubtful significance in view of the uncertainties in the value of the local viscosity and the large errors in experimentally determined T_1 and line width values.

Other collagen structures have been proposed (see Ramachandran, 1967) which differ in certain significant details from the poly(Gly-Pro-Pro) structure. However the $\theta_H{}^\alpha$ values for these structures are within 7° of the poly(Gly-Pro-Pro) angles, and hence, the R_2 values obtained using these other models are also consistent with experiment differing by less than 15% from the results in Table V.

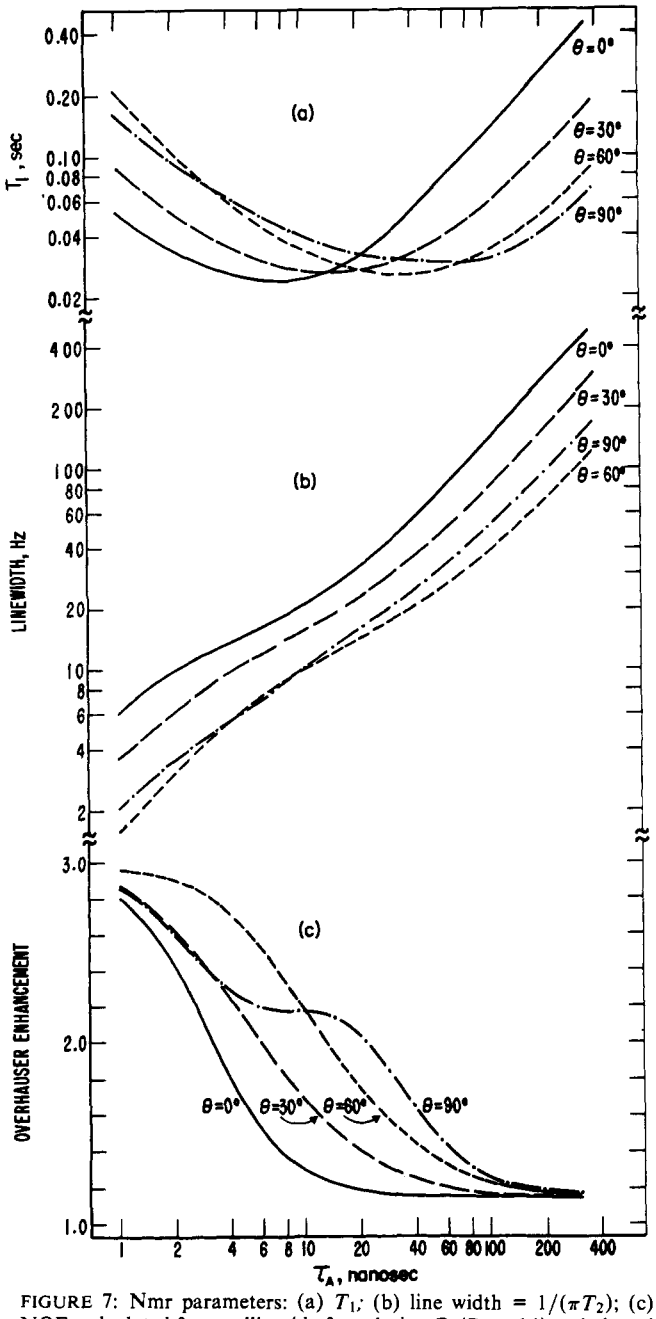

FIGURE 7: Nmr parameters: (a) T_1; (b) line width = $1/(\pi T_2)$; (c) NOE; calculated for an ellipsoid of revolution $R_1/R_2 = 14$) and plotted as a function of $\tau_A = (6R_2)^{-1}$ for $\theta = 0°$ (—), $\theta = 30°$ (- - -), $\theta = 60°$ (——), and $\theta = 90°$ (- · -), where θ is the angle made by the C–H internuclear vector with the symmetry axis of the helix. The curves apply to a carbon bonded to a single hydrogen with r_{CH} = 1.09 Å.

Side Chain Motion in the Helix. In globular proteins many side chains are buried and, as a consequence of the well-defined tertiary structure of the molecule, each such side chain has a well-defined conformation, which is specified by a set of torsion angles, χ^i, illustrated in Figure 8. If the side chains were rigid in the α1-CB2 helix, calculation of the relaxation times would follow the procedure used for the rigid C^α carbons in the helix backbone. However, in contrast with the globular proteins, all amino acid side chains in α1-CB2 are at the surface of the helix, and thus local motion is possible for all side chains. Analysis of the relaxation data is more difficult when local motion is present, with the complexity of the calculations depending on the details of the side chain motion (Woessner *et al.*, 1969;

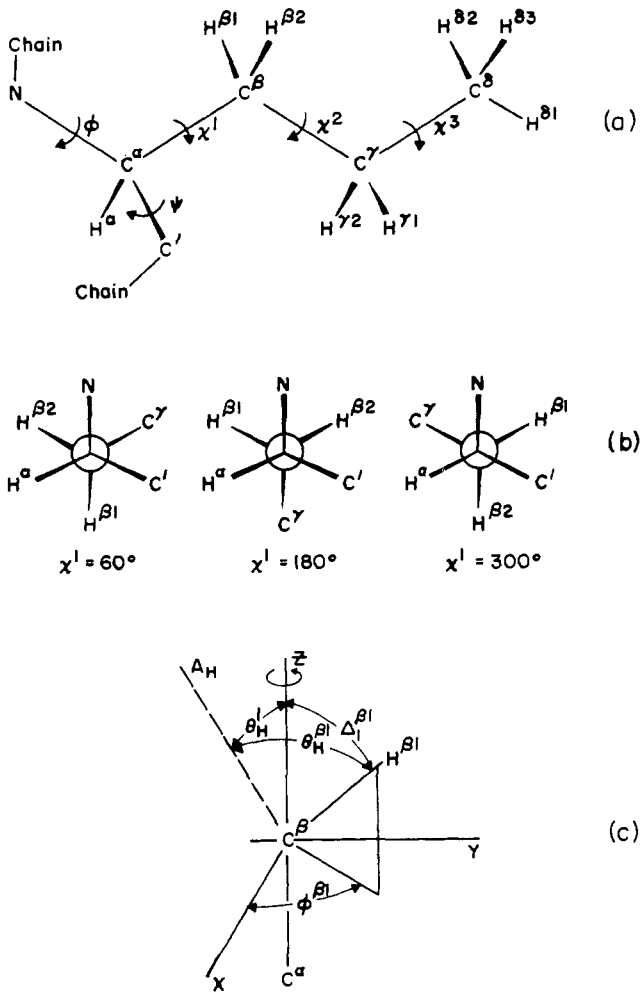

FIGURE 8: (a) The side chain torsional angles, χ^i, illustrated for a norvaline side chain in the extended conformation, $\chi^i = 180°$, $i = 1$-3; (b) $\chi^1 = 60$, 180, and 300°, the low energy rotamers of the C^{α}-C^{β} bond; (c) the angles needed to calculate nmr parameters when the χ^1 rotamers have unequal populations.

Wallach, 1967; Levine *et al.*, 1973). For instance, the motion of the C^{β} methyl moieties of the two Ala residues can be considered to result from rotational jumps between three equally populated rotational isomers, $\chi^1 = 60$, 180, and 300°. The rotation rate, R_{χ^1}, is much greater than R_1 and R_2 since a space filling (CPK[3]) model of α1-CB2 shows that there is no steric hindrance to methyl rotation. Under these conditions, and assuming that C^{β} valence angles are tetrahedral, Woessner's equations (Woessner *et al.*, 1969) reduce to the following simple expressions for the C^{β} T_1, line width, and NOE values

$$\begin{aligned} C^{\beta} - T_1 &= 3T_1(\tau_A, \theta_H{}^1) \\ C^{\beta} - \text{line width} &= \text{line width}(\tau_A, \theta_H{}^1)/3 \\ C^{\beta} - \text{NOE} &= \text{NOE}(\tau_A, \theta_H{}^1) \end{aligned} \quad (4)$$

The functions on the right-hand side of these equations are those plotted in Figure 7, and approximate values of τ_A (the helical correlation time) and $\theta_H{}^1$ (the angle between the helix axis and the C^{α}-C^{β} bond depicted in Figure 8c) are known. Earlier τ_A was shown to equal 130 nsec, while a value of $\theta_H{}^1 = 90°$ was calculated for the two Ala residues (both in the second position in their respective triplets) using the coordinates of the second residue in the poly(Gly-Pro-Pro) structure. Within experimental uncertainty, the measured values of the relaxation times (Table IV) agree with the values determined from the plots in Figure 7 using $\tau_A = 130$ nsec, $\theta_H{}^1 = 90°$ (Table IV).

The remaining α1-CB2 residue containing methyl groups is Leu(8) having two C^{δ} methyl carbons. Although it is in principle possible for Leu side chain motion to result from rotation about the C^{α}-C^{β} and C^{β}-C^{γ} bonds, the CPK model of the helix indicates that the only Leu side chain conformation free of steric contacts has $\chi^1 = 180°$, and $\chi^2 = 300°$. Hence, it is assumed that local reorientation of the Leu methyl groups is due to rotation about C^{γ}-$C^{\delta 1}$ and C^{γ}-$C^{\delta 2}$ bonds. These bonds make angles $\theta_H{}^{\delta 1} = 50°$ and $\theta_H{}^{\delta 2} = 60°$ with the helix axis (as calculated from the poly(Gly-Pro-Pro) backbone coordinates and $\chi^1 = 180°$ and $\chi^2 = 300°$) and using these values for the angular arguments in eq 4 yields relaxation times in agreement (Table IV) with the measured values.

The methyl carbon relaxation parameters are readily calculated because symmetry requires that the three rotational isomers must have equal populations. In the Phe residue, the C^{β}-C^{γ} bond is a C_2 symmetry axis for phenyl rotation, and both energy calculations (Ramachandran and Sasisekharan, 1968; Sasisekharan and Ponnuswamy, 1971) and X-ray data (Watson, 1968; Quiocho and Lipscomb, 1971) indicate that the $\chi^2 = 90$ and 270° are the isoenergetic lowest energy isomers. The space filling model of the helix indicates that phenyl rotation is possible only in the Phe $\chi^1 = 300°$ conformation. In the case of phenyl (χ^2) rotation, the angle between the Phe C^{δ}-H^{δ} (or the C^{ϵ}-H^{ϵ}) vector and the C^{β}-C^{γ} rotation axis (60°) is sufficiently close to the magic angle (54.7°) that the C^{δ} (or C^{ϵ}) T_1, line width, and NOE values can be calculated (Woessner *et al.*, 1969) as if the C^{δ}-H^{δ} and C^{ϵ}-H^{ϵ} vectors are undergoing isotropic reorientation with a correlation time, $\tau_{\chi^2} = 1/R_{\chi^2}$, where R_{χ^2} is the phenyl rotation rate. The measured Phe C^{δ} and C^{ϵ} T_1 values correspond to $\tau_{\chi^2} = 0.6$ nsec, but the measured line widths correspond to $\tau_{\chi^2} = 3$ nsec. This inconsistency arises because the $\chi^1 = 180$ and 60° rotamers were assumed to have zero populations in the calculations. A small population (≤20%) of these rotamers would have a large influence on the line width since phenyl rotation is hindered in these conformations.[9]

In contrast to the rather narrow lines observed for the Phe C^{δ} and C^{ϵ} resonances, the Phe C^{ζ} resonance is too broad to be resolved in the helix spectrum. This is so, since the C^{ζ}-H^{ζ} vector, which lies along the χ^2 rotation axis, is not reoriented by the χ^2 rotation, and the χ^1 rotation is not effective in reducing the C^{ζ} line width since—unlike methyl rotation—one χ^1 rotamer ($\chi^1 = 300°$) is predominantly populated.

The presence of unequally populated Phe χ^1 rotamers is not surprising since methylene moieties (unlike methyls) have asymmetric rotational potentials (Ramachandran and Sasisekharan, 1968; Sasisekharan and Ponnuswamy, 1971). X-Ray studies (Watson, 1968; Quiocho and Lipscomb, 1971) indicate that in globular proteins, the $\chi^1 = 300°$ rotational isomer is populated twice as frequently as the $\chi^1 = 180°$ rotamer, and with the exception of Ser (and Thr) the

[9] Hulmes *et al.* (1973) have suggested (on the basis of an analysis of the α1 sequence) that the stability of the staggered collagen fibril is due, in large measure, to interactions between large hydrophobic residues. The mobility exhibited by the Phe side chain in α1-CB2 implies that the phenyl ring projects out from the trimer surface, a result which provides experimental evidence that the Phe ring is in position to interact with large hydrophobic residues on other trimers.

polar residues are seldom observed to have $\chi^1 = 60°$. If one does assume χ^1 rotamers are equally populated in α1-CB2 and that $R_{\chi^1} \gg R_1$ then, calculated values of T_1 (0.1–0.15 sec) and line width (10–15 Hz) for β carbons differ greatly from the experimental values (Table IV). Calculation of the C^β relaxation times when rotamer populations are unequal involves many parameters—the rotamer populations, the rates of internal rotation and helix diffusion, and the angles $\theta_H{}^1$, $\phi^{\beta 1}$, and $\Delta^{\beta 1}$ defined in Figure 8c. Various combinations of the parameters yield approximately equal calculated values of T_1 and the line width. This fact coupled with the large uncertainties in the experimental T_1 and line width values means that, except for ruling out the presence of equally populated rotamers undergoing rapid reorientation, the present data cannot determine the rotation rates and rotamer populations of the linear side chains in α1-CB12. Similar circumstances preclude estimating the populations of the Pro ring conformations. The experimental situation regarding the Hyp residue is more favorable since the Hyp C^γ resonance (122.7 ppm) is well downfield of the aliphatic resonances. The large line width (50 Hz) and small T_1 value (0.04 sec) of the Hyp C^γ and the very broad Hyp C^β resonance at 155.5 ppm suggest that a single Hyp ring conformation is predominantly populated. This result is of interest in view of the recent evidence that the replacement of Hyp for Pro in the Gly-X-Pro triplet stabilizes the helix (Sakakibara *et al.*, 1973; Ward and Mason, 1973; Rosenbloom and Harsch, 1973; Berg and Prockop, 1973) presumably through an H-bond involving the C^γ–OH moiety.

Conclusions

The ^{13}C chemical shifts and relaxation times have provided a reasonably detailed picture of the structure and motion of the coil and helix forms of α1-CB2 in solution.[10] In the random coil, interior backbone carbons as well as terminal carbons and side chain carbons exhibit average rotational correlation times of <0.5 nsec. Due to the small line widths of the random coil, differences in molecular mobility of interior C^α carbons, near-terminal C^α carbons and side chain carbons of various types of residues can be distinguished. The rigid nature of the trimer is readily evident in the broad lines, small NOE values and small T_1 values measured at 2°. The measured relaxation times are consistent with those calculated for a rigid ellipsoid of revolution having dimensions and atomic coordinates expected for an α1-CB2 triple helix. The narrow lines present in the 2° spectrum are accounted for by the mobile residues in the terminal triplets of the helix and by the presence of a small amount of random coil α1-CB2 and α1-CB1. Local motion is also inferred from the nmr parameters measured for the side chains of the Ala, Leu, and Phe residues located in the interior of the sequence. Unfortunately, the question of local motion of other side chains cannot be answered with certitude, due to the overlap of the broad helical resonances which also produce the large uncertainties in the C^α relaxation times. Hence, information on the interactions involving side chains in the helix and the possible differences in orientation of C^α–H^α vectors with respect to the long axis of the helix cannot yet be attained. Two approaches to obtaining this more detailed information are ^{13}C labeling of specific residues, either biosynthetically or using the solid phase methods, and the use of high field (superconducting) spectrometers. These procedures will reduce or eliminate the problem of spectral overlap and thus permit accurate measurement of relaxation times for single carbons. Such results, coupled with extensions of available theories of side chain reorientation, should yield precise information regarding the motion of specific residues in the helix.

[10] Due to sensitivity limitations it was not possible to measure the ^{13}C nmr parameters with the α1-CB2 concentrations below 25 mg/ml. Proton line widths at 2° were found to be independent of concentration over the range 3–20 mg/ml. Also the α1-CB2 melting curve obtained by ORD at a concentration of 25 mg/ml was in accord with that predicted by the thermodynamic parameters of Piez and Sherman (1971b).

Acknowledgments

We are indebted to Professor D. F. DeTar and to Professor E. R. Blout for kindly providing the model polypeptides which were crucial in assigning the α1-CB2 resonances. We are grateful to Dr. K. A. Piez for his CPK model of the α1-CB2 helix and for encouragement and helpful discussions during the course of this work. Dr. D. VanderHart and Dr. H. M. McIntyre designed and built the Dewared probe which enabled long-term stable operation of the spectrometer system at 2°, and Mr. D. E. Brown provided expert technical assistance.

References

Abragam, A. (1961), The Principles of Nuclear Magnetism, London, Oxford University Press.

Allerhand, A., Doddrell, D., and Komoroski, R. (1971), *J. Chem. Phys. 55,* 189.

Berg, R. A., and Prockop, D. J. (1973), *Biophys. Biochem. Res. Commun. 52,* 115.

Berg, R. A., Kishida, Y., Kobayashi, Y., Inouye, K., Tonelli, A. E., Sakakibara, S., and Prockop, D. J. (1974), *Biochim. Biophys. Acta 328,* 553.

Bornstein, P. (1967), *Biochemistry 6,* 3082.

Bornstein, P., and Piez, K. A. (1966), *Biochemistry 5,* 3460.

Brown, F. R., III, diCorato, A., Lorenzi, G. P., and Blout, E. R. (1972), *J. Mol. Biol. 63,* 85.

Bovey, F. A., Brewster, A. I., Patel, D. J., Tonelli, A. E., and Torchia, D. A. (1972), *Accounts Chem. Res. 5,* 193, and references therein.

Butler, W., Piez, K. A., and Bornstein, P. (1967), *Biochemistry 6,* 3771.

Christl, M., and Roberts, J. D. (1972), *J. Amer. Chem. Soc. 94,* 4565.

Connor, T. M. (1963), *Trans. Faraday Soc. 60,* 1579.

Dorman, D. E., and Bovey, F. A. (1973), *J. Org. Chem. 38,* 2379, and references therein.

Epstein, E. H., Scott, R. D., Miller, E. J., and Piez, K. A. (1971), *J. Biol. Chem. 246,* 1718.

Farrar, T. C., and Becker, E. D. (1970), Pulse and Fourier Transform NMR, New York, N.Y., Academic Press.

Farrar, T. C., Druck, S. J., Shoup, R. R., and Becker, E. D. (1972), *J. Amer. Chem. Soc. 94,* 699.

Furthmayr, H., and Timpl, R. (1971), *Anal. Biochem. 41,* 510.

Goldstein, H. (1950), Classical Mechanics, Cambridge, Mass., Addison-Wesley, p 97.

Hulmes, D. J. S., Miller, A., Parry, D. A. D., Piez, K. A., and Woodhead-Galloway, J. (1973), *J. Mol. Biol. 79,* 137.

Inglis, A. S., and Edman, P. (1970), *Anal. Biochem. 37,* 73.

IUPAC-IUB Commission (1970), *Biochemistry 9,* 2471.

Kobayashi, Y., and Kyogoku, Y. (1973), *J. Mol. Biol. 81,*

337.
Kuhlmann, K., Grant, D. M., and Harris, R. K. (1970), *J. Chem. Phys. 52,* 3439.
Levine, Y. K., Partington, P.. and Roberts, G. C. K. (1973), *Mol. Phys. 25,* 497.
Levine, Y. K., Birdsall, N. J. M., Lee, A. G. Metcalfe, J. C., Partington, P., and Roberts, G. C. K. (1974), *J. Chem. Phys. 60,* 2890.
Lyerla, J. R., Jr., and Freedman, M. H. (1972), *J. Biol. Chem. 247,* 8183.
Lyerla, J. R., Jr., Barber, B. H., and Freedman, M. H. (1973), *Can. J. Biochem. 51,* 460.
Mattice, W. L., and Mandelkern, L. (1971), *Biochemistry 10,* 1934.
Perrin, F. (1936) *J. Phys. Radium 5,* 497.
Piez, K. A., and Sherman, M. R. (1970a), *Biochemistry 9,* 4129.
Piez, K. A., and Sherman, M. R. (1970b), *Biochemistry 9,* 4143.
Quiocho, F. A., and Lipscomb, W. N. (1971), *Advan. Protein Chem. 25,* 1.
Ramachandran, G. N. (1967), *in* Treatise on Collagen I. Chemistry of Collagen, Ramachandran, G. N., Ed., London, Academic Press, Chapter 3.
Ramachandran, G. N., and Sasisekharan, V. (1968), *Advan. Protein Chem. 23,* 283.
Rosenbloom, J., and Harsch, M. (1973), *Arch. Biochem. Biophys. 158,* 478.
Saito, H., and Smith, I. C. P. (1973), *Arch. Biochem. Biophys. 158,* 154.
Sakakibara, S., Inouye, K., Shudo, K., Kishida, Y., Kobayashi, Y., and Prockop, D. J. (1973), *Biochim. Biophys. Acta 303,* 198.
Sasisekharan, V., and Ponnuswamy, P. K. (1971), *Biopolymers 10,* 583.
Schaefer, J., and Natusch, D. F. S. (1972), *Macromolecules 5,* 416.
Solomon, I. (1955), *Phys. Rev. 99,* 559.
Torchia, D. A., and Piez, K. A. (1973), *J. Mol. Biol. 76,* 419.
Torchia, D. A., and Lyerla, J. R., Jr. (1974), *Biopolymers 13,* 97.
Torchia, D. A., Lyerla, J. R., Jr., and Quattrone, A. J. (1974a), Peptides, Polypeptides and Proteins, Blout, E. R., Bovey, F. A., Goodman, M., and Lotan, N., Ed., New York, N. Y., Wiley, p 436.
Torchia, D. A., Lyerla, J. R., Jr., and Deber, C. M. (1974b), *J. Amer. Chem. Soc. 96,* 5009, and references therein.
Traub, W., and Piez, K. A. (1971), *Advan. Protein Chem. 25,* 243.
Vold, R. L., Waugh, J. S., Klein, M. P., and Phelps, D. E. (1968), *J. Chem. Phys. 48,* 3831.
Wallach, D. (1967), *J. Chem. Phys. 47,* 5258.
Woessner, D. E. (1962), *J. Chem. Phys. 37,* 647.
Woessner, D. E., Snowden, B. S., Jr., and Meyer, G. H. (1969), *J. Chem. Phys. 50,* 719.
Ward, A. R., and Mason P. (1973), *J. Mol. Biol. 79,* 431.
Watson, H. C. (1968), *Progr. Stereochem. 4,* 299
Yonath, A., and Traub, W. (1969), *J. Mol. Biol. 43,* 461.

Reconstitution of Chromatin: Mode of Reassociation of Chromosomal Proteins†

Chi-Bom Chae

ABSTRACT: The mode of reassociation of Ehrlich ascites histones and non-histone proteins during chromatin reconstitution was studied by sodium dodecyl sulfate polyacrylamide gel electrophoresis. In the procedure of Bekhor et al. (I. Bekhor, G. M. Kung, and J. Bonner, (1969), *J. Mol. Biol. 39,* 351) most of histones and non-histone proteins reassociate with DNA in the last dialysis step of the dissociated chromatin, that is, the dialysis of the chromatin in 0.4 *M* NaCl–5 *M* urea against a dilute buffer. The reassociation of histones and non-histone proteins with DNA is more gradual in the procedure of L. Kleiman and R.-C. C. Huang [(1972), *J. Mol. Biol. 64,* 1]. However, in both procedures the bulk of the Ehrlich ascites non-histone proteins reassociate with DNA after the binding of histones to DNA. There are small amounts of non-histone proteins which reassociate with DNA before and at the same time as histones reassociate with DNA.

Chromatin consists of DNA, histones, non-histone proteins, and a small amount of RNA (Bonner et al., 1968). Isolated chromatin mediates the synthesis of tissue-specific RNAs in the presence of RNA polymerase (Axel et al., 1973; Gilmour and Paul, 1973; Steggles et al., 1974), and only a small portion of chromosomal DNA (2–10%) is transcribed into RNA in vivo (Grouse et al., 1972) and in vitro (Tan and Miyagi, 1970). Therefore, it appears that chromosomal proteins regulate the expression and repression of genes. Recently several reports have appeared on the reconstitution of fully dissociated chromatin, and the reconstituted chromatin appears to behave as native chromatin as far as the synthesis of tissue-specific RNAs is concerned (Bekhor et al., 1969; Huang and Huang, 1969; Spelsberg et al., 1971; Gilmour and Paul, 1970). The tissue specificity of chromatin seems to be controlled by non-histone proteins

† From the Department of Biochemistry, University of North Carolina, Chapel Hill, North Carolina 27514. *Received September 6, 1974.* Supported by U.S. Public Health Service General Research Support Award 5 S01-FR-05406.